Analysis of the August 2017 Eclipse's Effect on Radio Wave Propagation Employing a Raytrace Algorithm

M.L. Moses[1], L. Kordella[1], G.D. Earle[1], D. P. Drob[2], J. Huba[2] and S. Debchoudhury[1]

[1]Virginia Tech, [2]Naval Research Laboratory

Introduction

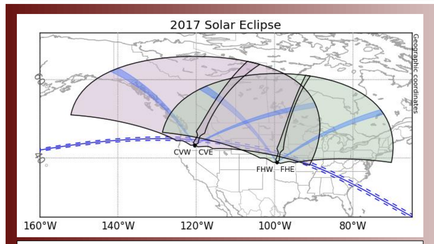

Figure 1. Eclipse path (blue) crossed SuperDARN fields of view (violet and green) and camping beams (indigo).

SuperDARN Operations

- The Super Dual Auroral Radar Network (SuperDARN) radars in Christmas Valley (CV), OR (violet) and Fort Hayes, KS (green) have Fields-of-View (FOVs) that covered part of the 2017 eclipse path (Fig.1).
- On eclipse day, these radars ran at ~10.5 MHz in every-other-beam mode.
  - 1 minute scan across radar's FOV.
  - Each radar made measurements on every-other beam, returning to the "camping" beam between successive beams.

SuperDARN Data

- The westward-looking radar at Christmas Valley (CVW) observed distinct variations in ionospheric propagation during the eclipse as seen in its camping beam's data (Fig. 2).
  - Increase in slant range during eclipse onset.
  - Relatively symmetric post-totality return to pre-eclipse conditions.
- These data's low velocities and spectral widths indicate that they are ground scatter, when a signal is refracted to Earth and then reflected back to the radar.

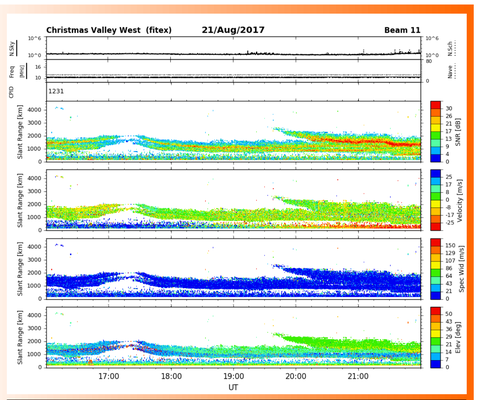

Figure 2. CVW beam 11 Range-Time-Intensity plots.

Initial Modeling

- The eclipse is modeled as a four dimensional (lat, lon, alt, time) accurate scaling of the NRL SAMI3 model's EUV flux. This eclipse mask is here referred to as the "Drob eclipse mask" and is described in more detail in Hairston *et al. (2018)*.
- Ray-trace through SAMI3's output and compare results to SuperDARN data at the modeled azimuths.

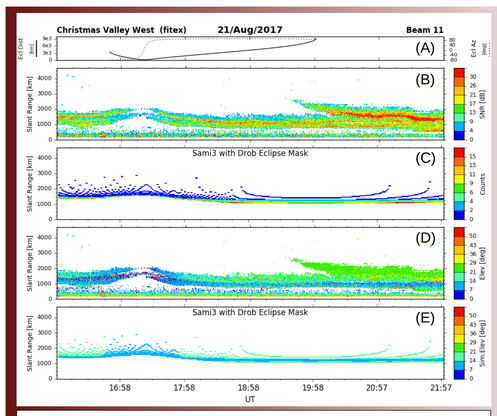

Figure 3. Raytrace output for SAMI3 eclipse model compared to measured data.

RTI Comparison Plots (top to bottom):

A. Eclipse geometry panel:
   - Left: Distance (km) of the eclipse center from radar
   - Right: Azimuth (degrees) of the eclipse center, relative to direct north from radar
B. Measured Signal-to-Noise ratio (SNR) of received signals.
C. The number of simulated rays in each range gate.
D. Measured angle-of-arrival for returned scatter.
E. Simulated initial elevation angle of ground scattered rays, assumed to be equivalent to angle-of-arrival.

Neutral Wind Study

Motivation

- As shown in Figure 3, the initial eclipse SAMI3 model matches the measured onset timescale and elevation angles fairly well; however, the model's recovery period is too long. This implies that some aspect of the model needs refinement.
- Possible causes of the model's inconsistency include the neutral wind velocity.
- Goal: Determine how neutral winds affect eclipse dynamics.

Methodology

- Employ SAMI2 to generate both uneclipsed and eclipsed (Drob eclipse mask) model ionospheres for different neutral wind velocities.
- Consider four cases: 1) no wind; 2) default wind values from the Horizontal-Wind-Model (HWM); 3) east/west wind values from HWM with no north/south wind; and 4) north/south wind values from HWM with no east/west wind.
- Use PHaRLAP to trace rays through the simulated medium. As the magnetic declination at CV is ~14.3º, our raytraces are run along beam 0 (16.74º) of the Christmas Valley East (CVE) radar.

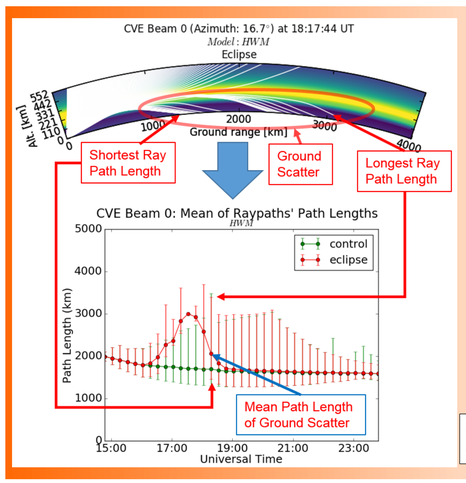

Figure 4. Example conversion from raytrace profile format to lineplot format.

Raytrace Lineplot

- For every time-step, we generate a raytrace profile plot (Fig. 4, top).
- For each ray that returns to Earth in that profile, we calculate the ray path length.
- We plot the average of these path lengths as a dot for each time. The range of path lengths is indicated by the vertical bars through each point.
- This process (illustrated in Fig. 4) is performed for both eclipse and control (uneclipsed) models, each with the same neutral winds.

Results

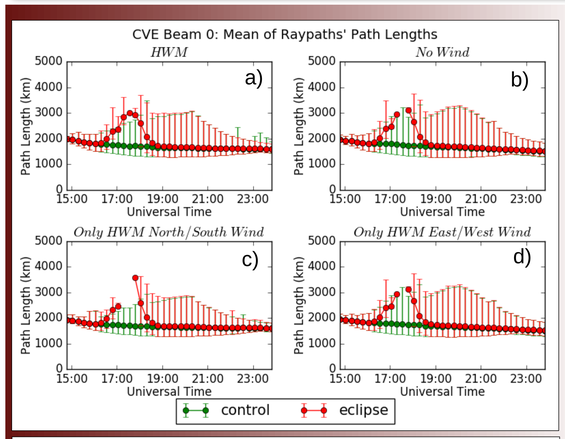

Figure 5. Raypath profile lineplots for four wind cases implemented in SAMI2.

- The "No Wind" case (Fig. 5b) and the "Only HWM East/West Wind" case (Fig. 5d) are very similar.
- The impact of the north/south wind (Fig.5c) is much more pronounced.
- The plots of Figure 5 show that the zonal (east/west) winds have a very small impact on the simulated radar data compared to that of the meridional (north/south) winds.

Discussion

- The drift velocity of species j due the neutral wind is

$$\vec{v}_{j,w} = \underbrace{\frac{\nu_j^2}{\omega_j^2+\nu_j^2}\vec{U}}_{(Pederson)} + \underbrace{\frac{\omega_j^2}{\omega_j^2+\nu_j^2}\frac{(\vec{U}\cdot\vec{B})\vec{B}}{|\vec{B}|^2}}_{(Direct)} + \underbrace{\frac{\nu_j\omega_j}{\omega_j^2+\nu_j^2}\frac{\vec{U}\times\vec{B}}{|\vec{B}|}}_{(Hall)}$$

$\vec{v}_{j,w}$: Drift Velocity due to Neutral Wind
ν_j: Collison Frequency
ω_j: Gyrofrequency
$\vec{U}$: Neutral Wind Velocity
$\vec{B}$: Magnetic Flux Density

- As shown above, drift velocity can be divided into three components, where each velocity component is categorized by its direction relative to $\vec{U}$ and $\vec{B}$.
- The relative magnitude of these components vary with gyrofrequency and ion-neutral collision frequency, which in turn vary with altitude.

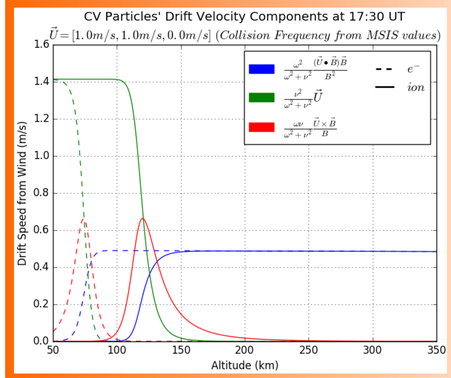

Figure 6. Magnitude of each component of the ion and electron drift velocities due to the neutral wind for a wind field that is 1m/s north and 1m/s east.

- As shown in Figure 6, at F-region altitudes the dominant component of the wind-driven drift velocity comes from the field-aligned (direct) component of the neutral wind.
- The magnetic declination at CV is about 14.3º. Hence, the meridional component of the neutral wind is more closely aligned with the magnetic field at CV than the zonal component.
- This supports our finding that the meridional wind has a greater effect on the simulation than does the zonal wind.
- Thus, the dominant drift velocity direction will be northward and downward for a northward wind.

Conclusions and Future Work

- The time of eclipse onset, the dip and the declination vary along the eclipse path. Since neutral winds vary with local time, the plasma dynamics in the recovery phase of the eclipse will depend on all of these variables.
- The meridional neutral wind velocity has a greater impact on the response observed than the zonal neutral wind velocity.
- SAMI and PHaRLAP can be used together to understand eclipse dynamics.
- The comparative model results may help to specify requirement constraints for future observational systems. Results of these future modeling studies should help to guide predictions for the 2024 eclipse.

References and Acknowledgments

Huba, J. D., and D. Drob (2017), SAMI3 prediction of the impact of the 21 August 2017 total solar eclipse on the ionosphere/plasmasphere system, *Geophysical Research Letters*, *44*(12), 5928-5935.

Rishbeth, H., and O. K. Garriott (1969), *Introduction to Ionospheric Physics*, Academic Press Inc. , New York; San Francisco; London.

Hairston, M. R., Mrak, S., Coley, W. R., Burrell, A., Holt, B., Perdue, M., ... & Power, R. (2018). Topside ionospheric electron temperature observations of the 21 August 2017 eclipse by DMSP spacecraft. *Geophysical Research Letters*, *45*(15), 7242-7247.

This work was supported by NSF Grant # AGS-1552188 and NASA Grant #NNX17AH70G.

The results presented in this poster were obtained using the HF propagation toolbox, PHaRLAP, created by Dr. Manuel Cervera, Defence Science and Technology Organisation, Australia (manuel.cervera@dsto.defence.gov.au). This toolbox is available by request from its author.

Joe Huba and Doug Drob, for SAMI3 output files used in raytrace simulation.

We acknowledge the use of the Free Open Source Software projects used in this analysis: Ubuntu Linux, Python, iPython, matplotlib, NumPy, SciPy, scikit-learn,Davitpy, and others.

Contact: magda14@vt.edu

CEDAR 2019